Research Article

Rutin pretreatment promotes microglial M1 to M2 phenotype polarization

Guang-Ping Lang[1], Can Li[1], Ying-Ying Han[2, *]

Graphical Abstract *Rutin switches microglial polarization from M1 to M2 to alleviate neuroinflammation*
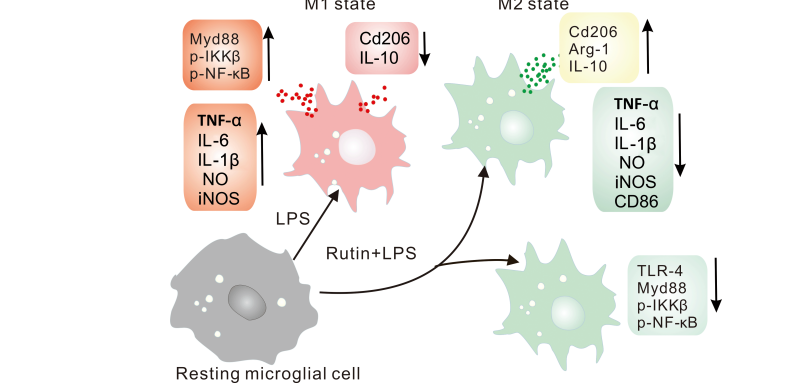
Abstract

Microglial cells are important resident innate immune components in the central nervous system that are often activated during neuroinflammation. Activated microglia can display one of two phenotypes, M1 or M2, which each play distinct roles in neuroinflammation. Rutin, a dietary flavonoid, exhibits protective effects against neuroinflammation. However, whether rutin is able to influence the M1/M2 polarization of microglia remains unclear. In this study, *in vitro* BV-2 cell models of neuroinflammation were established using 100 ng/mL lipopolysaccharide to investigate the effects of 1-hour rutin pretreatment on microglial polarization. The results revealed that rutin pretreatment reduced the expression of the proinflammatory cytokines tumor necrosis factor-α, interleukin-1β, and interleukin-6 and increased the secretion of interleukin-10. Rutin pretreatment also downregulated the expression of the M1 microglial markers CD86 and inducible nitric oxide synthase and upregulated the expression of the M2 microglial markers arginase 1 and CD206. Rutin pretreatment inhibited the expression of Toll-like receptor 4 and myeloid differentiation factor 88 and blocked the phosphorylation of I kappa B kinase and nuclear factor-kappa B. These results showed that rutin pretreatment may promote the phenotypic switch of microglia M1 to M2 by inhibiting the Toll-like receptor 4/nuclear factor-kappa B signaling pathway to alleviate lipopolysaccharide-induced neuroinflammation.
Key Words: BV-2 cells; flavonoid; M1 microglia; M2 microglia; microglia activation; microglia polarization; neuroinflammation; proinflammatory cytokines; rutin; TLR-4 signaling

Chinese Library Classification No. R453; R741; R285

Introduction

Neuroinflammation is significant in the central nervous system (CNS) (Yang et al., 2016; Mo et al., 2020). Microglial cells are resident immune cells, accounting for 15–20% of cranial nerve gliacytes in the CNS, which primarily function to remove injured nerves, cellular fragments, and infectious substances (Schneble et al., 2017). Microglial cells in the CNS tend to react early following infection, inflammation, and other pathophysiological stimuli (Hopp et al., 2018). Microglial cells can be converted from a surveillant state into an activated state upon CNS injury due to infection, cerebral trauma, or ischemia (Salvi et al., 2017; Huang et al., 2020). Microglial

activation results in alterations in cellular phenotypes and functions, and activated microglial cells typically demonstrate one of two distinct phenotypes, referred to as M1 and M2. M1 microglial cells can cause neurotoxicity by releasing cytotoxic substances and inflammatory factors, including matrix metalloproteinases that deteriorate the blood-brain barrier, further aggravating cerebral injury. Studies have found that M1 microglial cells can cause partial or extensive CNS injury, and the M1 phenotype serves as a histopathological marker for neurodegeneration, including Parkinson's disease and Alzheimer's disease (Hopp et al., 2018; Sternberg et al., 2019). Conversely, M2 microglial cells protect neurons by

[1]Key Laboratory of Basic Pharmacology of Ministry of Education and Joint International Research Laboratory of Ethnomedicine of Ministry of Education, Zunyi Medical University, Zunyi, Guizhou Province, China; [2]Special Key Laboratory of Oral Diseases Research, Higher Education Institutions of Guizhou Province, Zunyi Medical University, Zunyi, Guizhou Province, China
***Correspondence to:** Ying-Ying Han, PhD, hanyingying5219@163.com.
https://orcid.org/0000-0001-8426-0771 (Ying-Ying Han)

Research Article

secreting anti-inflammatory components and neurotrophic factors (Frister et al., 2014; Pisanu et al., 2014; Meireles et al., 2016). By interacting with Toll-like receptors (TLRs) on the cell surface, pathogen-associated molecular patterns can initiate microglial activation, converting microglial cells into the M1 proinflammatory phenotype (Frister et al., 2014). The stimulation of TLR4, which is primarily expressed on the cell surface of microglia in the CNS, activates the nuclear factor-kappa-B (NF-κB) signaling pathway, which is crucial for the activation of the M1 phenotype (Yin et al., 2018; Zhang et al., 2018b), resulting in the subsequent release of inflammatory factors that increase neuroinflammation and CNS injury. Previous studies have demonstrated that the conversion of microglia from an M1 to an M2 phenotype may serve as an effective approach to the control of neuroinflammation (Huang et al., 2016; Shabab et al., 2017; Li et al., 2018).

Rutin, which is also known as vitamin P, is a dietary flavonoid (Hollman and Katan, 1998). Clinically, rutin has been demonstrated to promote distinct pharmacological benefits, such as antioxidative, anti-inflammatory, and antiviral effects (Nafees et al., 2015). Rutin has been shown to protect the heart and kidney from injury caused by ischemia and inhibits apoptosis induced by myocardial ischemia (Jeong et al., 2009; Araújo et al., 2011). Importantly, rutin facilitates neuroprotection by activating antioxidative factors, including catalase, which reduces the formation of free radicals (Khan et al., 2009). Recent research has demonstrated that rutin can increase the expression of microglial cell phagocytic receptors, enhancing the clearance capability against β-amyloidosis, resulting in beneficial effects against the pathological progression of Alzheimer's disease (Wang et al., 2012; Pan et al., 2019). Both rutin and microglial activation appear to be involved in the neuroinflammatory response; however, whether rutin plays a role in the regulation of microglial phenotypic conversion remains unclear.

In the present study, we attempted to investigate whether rutin serves as an effective candidate for the promotion of microglial phenotypic conversion from M1 to M2 to further ameliorate neuroinflammation initiated by lipopolysaccharide (LPS) treatment in BV-2 microglial cells.

Materials and Methods

Cell culture and treatment
BV-2 microglial cells (purchased from China Center for Type Culture Collection) were cultured in high-glucose Dulbecco's modified Eagle medium (Thermo Fisher Scientific, Inc., Waltham, MA, USA) supplemented with 10% fetal bovine serum (BioInd, Inc., Shanghai, China) and 1% penicillin/streptomycin (Solarbio Science & Technology Co., Ltd., Beijing, China) under conditions of 37°C and 5% CO_2. Rutin (Solarbio Science & Technology Co., Ltd.) was dissolved in phosphate-buffered saline (containing 0.1% dimethyl sulfoxide, DMSO) and prepared as a 20 mg/mL stock solution. Rutin was diluted in Dulbecco's modified Eagle medium to the specified concentrations used in each experiment. The control group was treated with 0.1% dimethyl sulfoxide, which served as the vehicle control. LPS (Sigma-Aldrich, St. Louis, MO, USA) was dissolved in normal saline, prepared as a 50 µg/mL stock solution, and diluted in Dulbecco's modified Eagle medium to the specified concentrations used in each experiment. BV-2 cells in the control group were pretreated with DMSO, and cells in the experimental group were pretreated with rutin for 1 hour before stimulation with or without LPS (100 ng/mL) for 24 hours in the following experiments.

Cell viability assay
Cell counting kit-8 assay was performed to measure the viability of BV-2 cells. Cells (4×10^3 cells/well) were cultured in 96-well plates and pretreated with rutin at various concentrations (0, 6.25, 12.5, 25, 50, and 100 µg/mL) for 1

hour, followed by the addition of 100 ng/mL LPS or normal medium and incubation for 24 hours. Subsequently, 10 µL Cell Counting Kit-8 reagent (Dojindo, Shanghai, China) was added to each well and incubated at 37°C for 3 hours. The optical density at 450 nm was measured using a microplate reader (Thermo Fisher Scientific, Inc., Waltham, MA, USA).

Enzyme-linked immunosorbent assay
Cells were pretreated with rutin (12.5, 25, and 50 µg/mL) for 1 hour, followed by stimulation with or without LPS (100 ng/mL) for 24 hours. The concentrations of inflammatory factors, including tumor necrosis factor-α (TNF-α), interleukin (IL)-6, IL-1β, and IL-10, in the cell supernatants were measured using enzyme-linked immunosorbent assay (ELISA) kits (Servicebio Technology Co., Ltd., Wuhan, China), according to the manufacturer's instructions. The optical density at 450 nm was determined using a microplate reader.

Nitric oxide assay
The nitric oxide (NO) contents secreted by BV-2 cells were assessed using an NO test kit (Jiancheng, Nanjing, China). Briefly, cells were pretreated with 12.5, 25, and 50 µg/mL rutin for 1 hour, followed by stimulation with 0 or 100 ng/mL LPS for 24 hours. The concentrations of NO in cell supernatants were measured following the manufacturer's instructions.

Quantitative real-time polymerase chain reaction
An Axyprep total RNA preparation kit (AXYGEN Biosciences, Union City, CA, USA) and PrimeScript™ RT reagent kit (TaKaRa, Beijing, China) were used to perform total RNA extraction and reverse transcription, respectively. Relative mRNA expression levels were analyzed using the $2^{-\Delta\Delta Ct}$ method and normalized against the expression level of glyceraldehyde 3-phosphate dehydrogenase (*GAPDH*), which was used as a housekeeping gene. Murine *GAPDH* primer was obtained from Sangon Biotech (Shanghai, China). The following murine primer pairs were used: *CD86*: forward: 5′-ACG GAG TCA ATG AAG ATT TCC T-3′, reverse: 5′-GAT TCG GCT TCT TGT GAC ATA C-3′; *CD206* forward: 5V-CCT ATG AAA ATT GGG CTT ACG G-3′, reverse: 5′-CTG ACA AAT CCA GTT GTT GAG G-3′; inducible nitric oxide synthase (*iNOS*) forward: 5′-ACT CAG CCA AGC CCT CAC CTA C-3′, reverse: 5′-TCC AAT CTC TGC CTA TCC GTC TCG-3′.

Western blot assay
Cells were lysed in radioimmunoprecipitation assay buffer (Solarbio Science & Technology Co., Ltd.), the samples were centrifuged (12,000 r/min for 10 minutes at 4°C), and the protein concentrations were measured using a bicinchoninic acid protein assay (Generay Biotech Co., Ltd., Shanghai, China). After adding 5× protein sample buffer (Cat# P0015, Beyotime, Shanghai, China), lysates were heated to 95°C for 5 minutes. Protein samples were separated by 8% sodium dodecyl sulfate-polyacrylamide gel electrophoresis and then transferred to a polyvinylidene difluoride membrane. The membranes were blocked with 5% skimmed milk in phosphate-buffered saline containing Tween-20 for 2 hours at room temperature and immunoblotted overnight at 4°C with the following primary antibodies: rabbit monoclonal anti-CD86 antibody (1:1000, Cat# ab239075), goat polyclonal anti-arginase-1 (Arg-1) antibody (1:1000, Cat# ab60176), rabbit polyclonal anti-CD206 antibody (1:500, Cat# ab64693), rabbit polyclonal anti-iNOS antibody (1:1000, Cat# ab15323), rabbit polyclonal anti-TLR4 antibody (1:500, Cat# ab13556), rabbit monoclonal anti-inhibitor kappa B kinase β (IKK-β) antibody (1:500, Cat# ab32135), rabbit monoclonal anti-myeloid differentiation factor 88 (MyD88) antibody (1:1000, Cat# ab219413), rabbit polyclonal anti-NF-κB p65 antibody (1:1000, Cat# ab16502), rabbit monoclonal anti-p-IKK-β antibody (1:200, Cat# ab194519), rabbit polyclonal anti-p-NF-κB p65 antibody (1:1000, Cat# ab86299), and mouse monoclonal anti-β-actin antibody (1:5000, Cat# ab6276). All primary

antibodies were obtained from Abcam (Shanghai, China). The membrane was washed with Tris-buffered saline-Tween-20 and incubated with the appropriate horseradish peroxidase-conjugated secondary antibodies (goat anti-mouse IgG, Cat# A0216, 1:2000, Beyotime; goat anti-rabbit IgG, A0208, 1:2000, Beyotime; donkey anti-goat IgG, Cat# A0181, 1:2000, Beyotime) for 1 hour at room temperature. Protein bands were visualized with enhanced chemiluminescence substrate (Beyotime) and quantified using FujiFilm Multi Gauge Ver. 3.0 software (Fuji Photo Film Co., Tokyo, Japan). CD86, iNOS, Arg-1, and CD206 are critical markers for microglial polarization, whereas the remaining proteins are key components of the NF-κB pathway, which is closely associated with inflammation.

Immunofluorescence staining
Coverslips were coated for 2 hours by poly-L-lysine (0.1 mg/mL; Beyotime) at 37°C then placed into a 12-well plate. BV-2 cells were cultured on the coverslips at 75,000 cells/well and pretreated with rutin (12.5, 25 and 50 μg/mL) for 1 hour, followed by incubation with LPS (100 ng/mL) for 24 hours. The cells were fixed with 4% paraformaldehyde for 30 minutes at room temperature, followed by permeabilization with 0.3% Triton X-100 for 15 minutes. Cells were subsequently blocked with 2% bovine serum albumin in phosphate-buffered saline at 37°C for 1 hour and incubated with individual antibodies: anti-CD86 (1:50) and anti-Arg-1 (1:50) at 4°C overnight. Subsequently, the cells were incubated with the appropriate secondary antibody (cyanine 3-conjugated donkey anti-rabbit IgG, Cat# GB21403, 1:500, Solarbio Science & Technology Co., Ltd.; fluorescein isothiocyanate conjugated donkey anti-goat IgG, Cat# GB22404; 1:500, Solarbio Science & Technology Co., Ltd.) for 2 hours at room temperature, followed by incubation with 4′,6-diamidino-2-phenylindole for 2 minutes at room temperature. The coverslips were mounted and examined under a fluorescence microscope (Olympus, Tokyo, Japan) at 20× magnification.

Statistical analysis
All data are presented as the mean ± standard error of the mean (SEM) after analysis with GraphPad Prism software v5.01 (GraphPad Software Inc., San Diego, CA, USA). Comparisons between groups were analyzed by one-way analysis of variance, and *post hoc* comparisons were made using Tukey's multiple comparison test. When $P < 0.05$, the difference was considered significant.

Results

Effects of rutin on LPS-induced BV-2 microglial cell morphology
To assess the potential cytotoxicity induced by rutin treatment in BV-2 cells, a Cell Counting Kit-8 experiment was performed. The viability of BV-2 cells was evaluated following treatments with various concentrations of rutin for 1 hour. The results indicated that BV-2 cell viability was significantly enhanced after rutin (12.5, 25, and 50 μg/mL) administration ($P < 0.05$) compared with cells treated with vehicle control. Therefore, these concentrations of rutin (12.5, 25, and 50 μg/mL) were selected for the subsequent experiments. No perceptible cytotoxicity was observed in BV-2 cells following 1-hour rutin treatment at concentrations ranging from 0 to 100 μg/mL (**Figure 1A**). Upon incubation with 100 ng/mL LPS for an additional 24 hours, BV-2 cell viability continued to remain unaffected (**Figure 1B**). As shown in **Figure 1C**, cells stimulated with LPS demonstrated an activated phenotype, characterized by elongated branches, whereas BV-2 cells in the unstimulated control group showed small cell bodies, and rutin pretreatment at concentrations of 25 and 50 μg/mL attenuated LPS-induced morphological alterations in BV-2 cells (**Figure 1C**). These data suggested that rutin exerts an important function during LPS-induced BV-2 cell activation.

Rutin affects LPS-induced inflammatory mediator production from BV-2 cells
BV-2 cells were first pretreated with various rutin concentrations (12.5, 25, and 50 μg/mL) for 1 hour before incubation with 100 ng/mL LPS for 24 hours. The concentrations of inflammatory cytokines in the supernatants were measured by ELISA. Following LPS treatment, TNF-α, IL-1β, IL-6, and NO concentrations were significantly increased ($P < 0.05$) compared with the unstimulated control, which indicated the potential M1 proinflammatory polarization of BV-2 cells in response to LPS stimulation (**Figure 2A–D**). However, the IL-10 level was not greatly altered by LPS treatment (**Figure 2E**). As expected, the TNF-α, IL-1β, IL-6, and NO concentrations induced by LPS treatment were dramatically reduced by rutin pretreatment at certain concentrations or concentration ranges (**Figure 2A–D**). In contrast, 50 μg/mL rutin pretreatment significantly elevated the expression level of the typical M2-associated anti-inflammatory cytokine IL-10 (**Figure 2E**). These results indicated that rutin treatment might facilitate the microglial cell conversion from a proinflammatory M1 to an anti-inflammatory M2 phenotype.

Rutin promotes the microglial phenotypic switch from M1 to M2
To further examine whether rutin contributes to BV-2 cell polarization to promote the anti-inflammatory M2 phenotype following LPS stimulation, we further evaluated the expression of iNOS, CD86, CD206, and Arg-1 in rutin-treated cells. Our immunofluorescence staining results revealed that BV-2 cells displayed enhanced CD86 immunopositivity after LPS stimulation compared with that in the control group, but the production of Arg-1 in BV-2 cells was not dramatically influenced by LPS stimulation (**Figure 3A** and **B**). The increase in CD86 immunopositivity induced by LPS stimulation was inhibited by rutin pretreatment, whereas Arg-1 immunopositivity was slightly increased in the rutin pretreatment group (50 μg/mL). In addition, when compared with those cells only exposed to LPS, western blot quantification data revealed that rutin-pretreated BV-2 cells expressed increased levels of Arg-1 and CD206 and decreased levels of CD86 and iNOS (**Figure 3C**). The corresponding representative western blotting image is shown in **Figure 3D**. We then examined the effects of rutin pretreatment on microglial polarization following LPS stimulation at the transcriptional level. The expression of CD86 and iNOS were significantly increased, whereas CD206 expression was significantly decreased in LPS-stimulated cells. Among these three markers, only iNOS mRNA expression was inhibited in the rutin pretreatment groups (**Figure 3E**). These results further suggested that rutin is capable of shifting LPS-induced BV-2 cell polarization from the M1 to the M2 phenotype.

Rutin inhibits activation of TLR4/NF-κB triggered by LPS in BV-2 cells
BV-2 cells were treated as described above. To explore which signaling pathways rutin acts on to promote the M1 to M2 polarization of BV-2 cells, the expression levels of TLR4, MyD88, IKK-β, NF-κB, p-IKK-β, p65, and p-NF-κB p65 were determined by western blot analysis. As expected, TLR4 and MyD88 protein expression levels were enhanced after LPS stimulation, whereas rutin treatment effectively reversed this upregulation in BV-2 cells. We subsequently tested the activation of IKK-β and NF-κB p65 by examining their phosphorylated states. Increased expression levels of p-IKK-β and p-NF-κB p65 can be observed following LPS stimulation, which was attenuated by rutin pretreatment (**Figure 4**). These results suggested that the activation of the TLR4/NF-κB, triggered by LPS stimulation in BV-2 cells, was limited by rutin pretreatment *in vitro*.
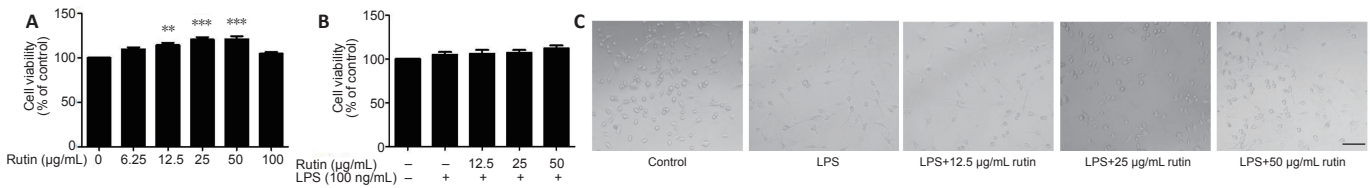
Figure 1 | Effects of rutin on BV-2 microglial cells stimulated with LPS.
(A) Viability of BV-2 cells after treatment with rutin (0, 6.25, 12.5, 25, 50, and 100 μg/mL) for 1 hour. (B) Viability of BV-2 cells after 1 hour of pretreatment with rutin at concentrations of 0, 12.5, 25, and 50 μg/mL, together with 24 hours of LPS stimulation (100 ng/mL). The viability of BV-2 cells was evaluated by Cell Counting Kit-8, and absorbance was examined by a microplate reader at 450 nm. Data are expressed as the mean ± SEM of 6 individual experiments for each group. **$P < 0.01$, ***$P < 0.001$ (one-way analysis of variance followed by Tukey's *post hoc* test). (C) BV-2 cell morphological changes stimulated by treatment with LPS alone or combined with rutin pretreatment. Pretreatment with rutin at 25 and 50 μg/mL reversed LPS-induced morphological alterations in BV-2 cells. Scale bar: 100 μm. LPS: Lipopolysaccharide.
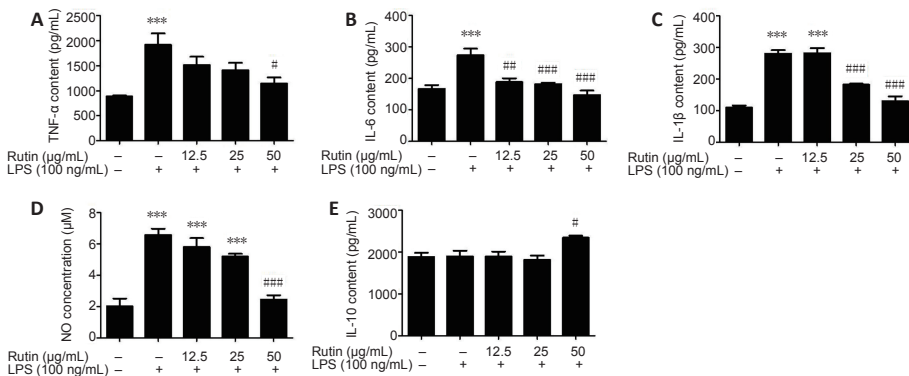
Figure 2 | Effects of rutin on LPS-induced inflammatory mediator production in BV-2 cells.
BV-2 cells were pretreated with 12.5, 25, and 50 μg/mL rutin for 1 hour, followed by 100 ng/mL LPS stimulation for 24 hours. (A–E) Quantification of cytokine and NO levels in the supernatants, performed by enzyme-linked immunosorbent assay. Data are expressed as the mean ± SEM of 5 (A–C and E) or 6 (D) individual experiments for each group. ***$P < 0.001$, *vs.* control group; #$P < 0.05$, ##$P < 0.01$, ###$P < 0.001$, *vs.* LPS-stimulated group (one-way analysis of variance followed by Tukey's *post hoc* test). IL: interleukin; LPS: lipopolysaccharide; NO: nitric oxide; TNF-α: tumor necrosis factor-α.
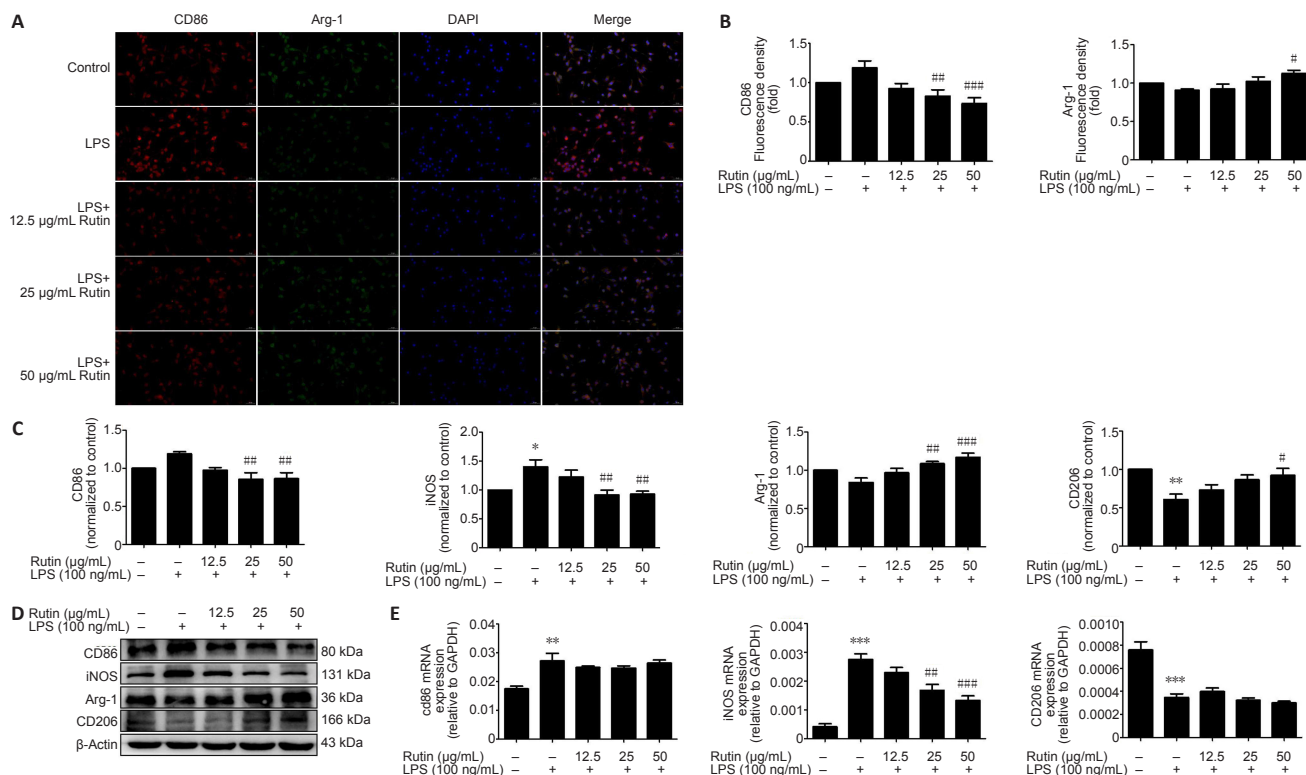
Figure 3 | Rutin switches microglial polarization from the M1 to M2 state in LPS-induced BV-2 cells.
BV-2 cells were pretreated with 12.5, 25, and 50 μg/mL rutin for 1 hour, followed by 100 ng/mL LPS stimulation for 24 hours. (A) Fluorescence images stained with anti-CD86 (red, stained by Cy3) and anti-Arg-1 (green, stained by fluorescein isothiocyanate) antibodies, and a blue-fluorescent DNA stain, DAPI. Images show that rutin pretreatment limits LPS-stimulated CD86 expression and enhances Arg-1 expression. Scale bars: 50 μm. (B) Fluorescence intensity quantification for CD86 and Arg-1. (C) CD86, Arg-1, iNOS, and CD206 protein expression levels were measured by western blot analysis. β-Actin was the loading control. (D) A representative western blot out of five independent experiments is shown. (E) mRNA expression levels for CD86, iNOS, and CD206 in BV-2 cells were detected by quantitative real-time polymerase chain reaction. Data are expressed as the mean ± SEM of 6 (A–D) or 5 (E) individual experiments for each group. *$P < 0.05$, **$P < 0.01$, ***$P < 0.001$, *vs.* control group; #$P < 0.05$, ##$P < 0.01$, ###$P < 0.001$, *vs.* LPS-stimulated group (one-way analysis of variance followed by Tukey's *post hoc* test). Arg-1: Arginase-1; DAPI: 4′,6-diamidino-2-phenylindole; iNOS: inducible nitric oxide synthase; LPS: lipopolysaccharide.
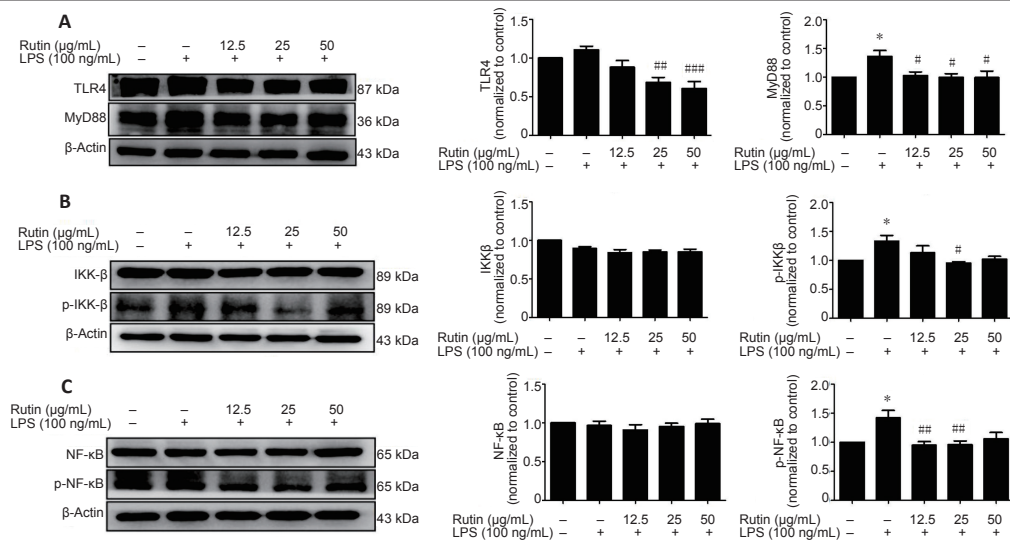
Figure 4 | Rutin inhibits the LPS-triggered TLR4/NF-κB activation in BV-2 cells.

BV-2 cells were pretreated with 12.5, 25, and 50 μg/mL rutin for 1 hour, followed by 100 ng/mL LPS stimulation for 24 hours. The expression levels of (A) TLR4 and MyD88, (B) IKK-β and p-IKK-β, and (C) NF-κB p65 and p-NF-κB p65 in BV-2 cells were analyzed by western blot analysis, and representative western blots are shown. Data are expressed as the mean ± SEM of 5 individual experiments for each group. *$P < 0.05$, vs. control group; #$P < 0.05$, ##$P < 0.01$, ###$P < 0.001$, vs. LPS-stimulated group (one-way analysis of variance followed by Tukey's post hoc test). IKK-β: Inhibitor kappa B kinase β; LPS: lipopolysaccharide; MyD88: myeloid differentiation factor 88; NF-κB: nuclear factor-kappa-B; TLR4: Toll-like receptor 4.

Discussion

The present investigation discovered that rutin promotes the transition of microglial polarization from the M1 to the M2 state, which has the potential to ease neuroinflammation. Our findings showed that rutin inhibits the expression of CD86 and iNOS and increases the expression of CD206 and Arg-1; however, rutin has no regulatory effects on CD86 and CD206 at the transcriptional level, indicating that rutin may play a post-transcriptional regulatory for these two microglial polarization-related proteins. As expected, rutin significantly reduced IL-6, TNF-α, IL-1β, and NO expression in BV-2 microglial cells after LPS stimulation but significantly enhanced IL-10 expression, suggesting a protective effect for rutin during neuroinflammation. Studies have described the upregulation of iNOS when microglial cells switch to the M1 phenotype (Cunha et al., 2016; Zhao et al., 2019). The iNOS and NO concentrations were consistently decreased by rutin, which is significant in terms of microglial polarization. Moreover, our results suggested that rutin pretreatment significantly inhibited the activation of TLR4/NF-κB signaling, implying that NF-κB signaling might be an important target for rutin during this biological process.

A phenotypic switch between the M1- and M2-dominant inflammatory response can occur in both microglia and macrophages under certain conditions. To maintain homeostasis, a careful balance must be maintained between the M1 and M2 microglial states (Zhang et al., 2018a). In the tumor microenvironment, the proinflammatory cytokines TNF-α and IL-1β and the bacterial LPS can upregulate iNOS production, triggering high levels of NO production, which has been associated with tumor growth (Lamagna et al., 2006; Nath and Kashfi, 2020). In studies performed on co-cultures containing glioblastoma and primary microglial cells, microglia-derived iNOS and NO levels were upregulated, resulting in enhanced microglial phagocytosis (Korbelik et al., 2000). Microglial phagocytosis capabilities were also improved by exogenous NO intervention (Kreutzberg, 1995). Similar to the outcome observed for tumor conditions, intracellular iNOS and extracellular NO concentrations increased when BV-2 microglia were stimulated with LPS in our study. The upregulation in both iNOS and NO production could be downregulated by rutin pretreatment, which suggested that rutin may inhibit microglia-mediated neuroinflammation via an NO-dependent mechanism. Other studies have shown that NO-mediated mechanisms are critical for M1 macrophage pathology in Duchenne muscular dystrophy and tumors (Villalta et al., 2009; Mukherjee et al., 2016). Consistently, our results suggest that rutin facilitated the microglial polarization from an M1 to an M2 phenotype through a mechanism associated with the downregulation of NO. Elevated NO was shown to provoke neuroinflammation in neurodegenerative diseases by regulating axonal degeneration and activating cyclooxygenases (Tse, 2017). In tumor biology, scientists have viewed the phenotypic switching of macrophages from M2 to M1 as a potential method for enhancing anti-tumor capabilities (Nath and Kashfi, 2020), which could be mediated by controlling NO-involved signaling. Similarly, our results indicated that rutin might be a promising candidate for the treatment of neurological disorders by promoting the phenotypic switching of microglia from the M1 to M2 state.

LPS has been well-established to activate TLR4 and induce microglial M1-phenotypic polarization with proinflammatory functions. Therefore, LPS-stimulated BV-2 microglial cells were employed to investigate whether rutin plays a role in microglial phenotypic switching. In the tumor microenvironment, the NF-κB pathway has been found to regulate macrophage polarization in mice (Kono et al., 2014). NF-κB signaling has been found to be critical for microglial phenotypic transformations both in vivo and in vitro in Alzheimer's disease (Wang et al., 2015; Ślusarczyk et al., 2018). Similar to previous work, our findings revealed that TLR4, MyD88, p-IKK-β, and p-NF-κB p65 expression levels were decreased by rutin pretreatment, resulting in microglial polarization directed toward the M2 state. Our data indicated that rutin might regulate microglial polarization via the suppression of TLR4/NF-κB signaling. However, our current data were unable to confirm whether rutin promotes the microglial M2 phenotype through the TLR4/NF-κB pathway because other pathways, such as Notch signaling and glycogen synthase kinase 3 signaling, could also be modulated by rutin during this process. Notch signaling inhibition has been shown to limit M1 marker expression and elevates M2 microglial polarization following LPS administration in BV-2 cells (Zhang et al., 2017). In addition, the expression level of the neuroprotective cytokine IL-10 was upregulated by rutin in our study, and regulatory T lymphocytes have been shown to ameliorate intracerebral hemorrhage-induced inflammatory injury by promoting microglial cell conversion to the M2 phenotype through the IL-10/GSK3β/phosphatase and tensin homolog axis (Zhou et al., 2017). Collectively, our results imply that rutin could represent a promising therapeutic candidate for neuroinflammatory diseases by promoting the microglia conversion from the M1 to M2 phenotype via effects on TLR4/NF-κB signaling. However, further investigations, including experiments performed in primary microglia and animal models, remain necessary to understand the role played by

rutin on microglial polarization.

In summary, the present study illustrated that rutin is capable of shifting the microglial state from the M1 to M2 phenotypes, attenuating microglia-related neuroinflammation. Moreover, this study revealed that the TLR4/NF-κB signaling might be involved in the rutin-mediated phenotypic shift of microglia. Therefore, our findings offer evidence that rutin might represent an effective therapeutic candidate for the treatment of neuroinflammatory diseases. However, whether rutin acts directly on the TLR4/NF-κB pathway or indirectly regulates the expression of TLR4 or NF-κB to influence the microglial M1 to M2 phenotype polarization remains to be tested.

References

Araújo JR, Gonçalves P, Martel F (2011) Chemopreventive effect of dietary polyphenols in colorectal cancer cell lines. Nutr Res 31:77-87.

Cunha C, Gomes C, Vaz AR, Brites D (2016) Exploring new inflammatory biomarkers and pathways during LPS-induced M1 polarization. Mediators Inflamm 2016:6986175.

Frister A, Schmidt C, Schneble N, Brodhun M, Gonnert FA, Bauer M, Hirsch E, Müller JP, Wetzker R, Bauer R (2014) Phosphoinositide 3-kinase γ affects LPS-induced disturbance of blood-brain barrier via lipid kinase-independent control of cAMP in microglial cells. Neuromolecular Med 16:704-713.

Hollman PC, Katan MB (1998) Bioavailability and health effects of dietary flavonols in man. Arch Toxicol Suppl 20:237-248.

Hopp SC, Lin Y, Oakley D, Roe AD, DeVos SL, Hanlon D, Hyman BT (2018) The role of microglia in processing and spreading of bioactive tau seeds in Alzheimer's disease. J Neuroinflammation 15:269.

Huang C, Liu YB, Dai YP, Wang LL, Cui YH, Yang JD (2020) Transplantation of bone marrow mesenchymal stem cells overexpressing glial cell line derived neurotrophic factor gene for spinal cord injury. Zhongguo Zuzhi Gongcheng Yanjiu 24:1037-1045.

Huang HY, Chang HF, Tsai MJ, Chen JS, Wang MJ (2016) 6-Mercaptopurine attenuates tumor necrosis factor-α production in microglia through Nur77-mediated transrepression and PI3K/Akt/mTOR signaling-mediated translational regulation. J Neuroinflammation 13:78.

Jeong JJ, Ha YM, Jin YC, Lee EJ, Kim JS, Kim HJ, Seo HG, Lee JH, Kang SS, Kim YS, Chang KC (2009) Rutin from Lonicera japonica inhibits myocardial ischemia/reperfusion-induced apoptosis in vivo and protects H9c2 cells against hydrogen peroxide-mediated injury via ERK1/2 and PI3K/Akt signals in vitro. Food Chem Toxicol 47:1569-1576.

Khan MM, Ahmad A, Ishrat T, Khuwaja G, Srivastawa P, Khan MB, Raza SS, Javed H, Vaibhav K, Khan A, Islam F (2009) Rutin protects the neural damage induced by transient focal ischemia in rats. Brain Res 1292:123-135.

Kono Y, Kawakami S, Higuchi Y, Maruyama K, Yamashita F, Hashida M (2014) Tumour-associated macrophages targeted transfection with NF-κB decoy/mannose-modified bubble lipoplexes inhibits tumour growth in tumour-bearing mice. J Drug Target 22:439-449.

Korbelik M, Parkins CS, Shibuya H, Cecic I, Stratford MR, Chaplin DJ (2000) Nitric oxide production by tumour tissue: impact on the response to photodynamic therapy. Br J Cancer 82:1835-1843.

Kreutzberg GW (1995) Microglia, the first line of defence in brain pathologies. Arzneimittelforschung 45:357-360.

Lamagna C, Aurrand-Lions M, Imhof BA (2006) Dual role of macrophages in tumor growth and angiogenesis. J Leukoc Biol 80:705-713.

Li C, Zhang C, Zhou H, Feng Y, Tang F, Hoi MPM, He C, Ma D, Zhao C, Lee SMY (2018) Inhibitory effects of betulinic acid on LPS-induced neuroinflammation involve M2 microglial polarization via CaMKKβ-dependent AMPK activation. Front Mol Neurosci 11:98.

Meireles M, Marques C, Norberto S, Santos P, Fernandes I, Mateus N, Faria A, Calhau C (2016) Anthocyanin effects on microglia M1/M2 phenotype: Consequence on neuronal fractalkine expression. Behav Brain Res 305:223-228.

Mo Y, Sun YY, Liu KY (2020) Autophagy and inflammation in ischemic stroke. Neural Regen Res 15:1388-1396.

Mukherjee S, Baidoo J, Fried A, Atwi D, Dolai S, Boockvar J, Symons M, Ruggieri R, Raja K, Banerjee P (2016) Curcumin changes the polarity of tumor-associated microglia and eliminates glioblastoma. Int J Cancer 139:2838-2849.

Nafees S, Rashid S, Ali N, Hasan SK, Sultana S (2015) Rutin ameliorates cyclophosphamide induced oxidative stress and inflammation in Wistar rats: role of NFκB/MAPK pathway. Chem Biol Interact 231:98-107.

Nath N, Kashfi K (2020) Tumor associated macrophages and 'NO'. Biochem Pharmacol 176:113899.

Pan RY, Ma J, Kong XX, Wang XF, Li SS, Qi XL, Yan YH, Cheng J, Liu Q, Jin W, Tan CH, Yuan Z (2019) Sodium rutin ameliorates Alzheimer's disease-like pathology by enhancing microglial amyloid-β clearance. Sci Adv 5:eaau6328.

Pisanu A, Lecca D, Mulas G, Wardas J, Simbula G, Spiga S, Carta AR (2014) Dynamic changes in pro- and anti-inflammatory cytokines in microglia after PPAR-γ agonist neuroprotective treatment in the MPTPp mouse model of progressive Parkinson's disease. Neurobiol Dis 71:280-291.

Salvi V, Sozio F, Sozzani S, Del Prete A (2017) Role of atypical chemokine receptors in microglial activation and polarization. Front Aging Neurosci 9:148.

Schneble N, Schmidt C, Bauer R, Müller JP, Monajembashi S, Wetzker R (2017) Phosphoinositide 3-kinase γ ties chemoattractant- and adrenergic control of microglial motility. Mol Cell Neurosci 78:1-8.

Shabab T, Khanabdali R, Moghadamtousi SZ, Kadir HA, Mohan G (2017) Neuroinflammation pathways: a general review. Int J Neurosci 127:624-633.

Ślusarczyk J, Trojan E, Głombik K, Piotrowska A, Budziszewska B, Kubera M, Popiołek-Barczyk K, Lasoń W, Mika J, Basta-Kaim A (2018) Targeting the NLRP3 inflammasome-related pathways via tianeptine treatment-suppressed microglia polarization to the M1 phenotype in lipopolysaccharide-stimulated cultures. Int J Mol Sci 19:1965.

Sternberg Z, Podolsky R, Nir A, Yu J, Nir R, Halvorsen SW, Chadha K, Quinn JF, Kaye J, Kolb C (2019) Increased free prostate specific antigen serum levels in Alzheimer's disease, correlation with cognitive decline. J Neurol Sci 400:188-193.

Tse JKY (2017) Gut microbiota, nitric oxide, and microglia as prerequisites for neurodegenerative disorders. ACS Chem Neurosci 8:1438-1447.

Villalta SA, Nguyen HX, Deng B, Gotoh T, Tidball JG (2009) Shifts in macrophage phenotypes and macrophage competition for arginine metabolism affect the severity of muscle pathology in muscular dystrophy. Hum Mol Genet 18:482-496.

Wang S, Jing H, Yang H, Liu Z, Guo H, Chai L, Hu L (2015) Tanshinone I selectively suppresses pro-inflammatory genes expression in activated microglia and prevents nigrostriatal dopaminergic neurodegeneration in a mouse model of Parkinson's disease. J Ethnopharmacol 164:247-255.

Wang SW, Wang YJ, Su YJ, Zhou WW, Yang SG, Zhang R, Zhao M, Li YN, Zhang ZP, Zhan DW, Liu RT (2012) Rutin inhibits β-amyloid aggregation and cytotoxicity, attenuates oxidative stress, and decreases the production of nitric oxide and proinflammatory cytokines. Neurotoxicology 33:482-490.

Yang XW, Li YH, Zhang H, Zhao YF, Ding ZB, Yu JZ, Liu CY, Liu JC, Jiang WJ, Feng QJ, Xiao BG, Ma CG (2016) Safflower Yellow regulates microglial polarization and inhibits inflammatory response in LPS-stimulated Bv2 cells. Int J Immunopathol Pharmacol 29:54-64.

Yin D, Zhou S, Xu X, Gao W, Li F, Ma Y, Sun D, Wu Y, Guo Q, Liu H, Han L, Wang Z, Wang Y, Zhang J (2018) Dexmedetomidine attenuated early brain injury in rats with subarachnoid haemorrhage by suppressing the inflammatory response: The TLR4/NF-κB pathway and the NLRP3 inflammasome may be involved in the mechanism. Brain Res 1698:1-10.

Zhang B, Wei YZ, Wang GQ, Li DD, Shi JS, Zhang F (2018a) Targeting MAPK pathways by naringenin modulates microglia M1/M2 polarization in lipopolysaccharide-stimulated cultures. Front Cell Neurosci 12:531.

Zhang F, Zhong R, Li S, Fu Z, Cheng C, Cai H, Le W (2017) Acute hypoxia induced an imbalanced M1/M2 activation of microglia through NF-κB signaling in Alzheimer's disease mice and wild-type littermates. Front Aging Neurosci 9:282.

Zhang L, Previn R, Lu L, Liao RF, Jin Y, Wang RK (2018b) Crocin, a natural product attenuates lipopolysaccharide-induced anxiety and depressive-like behaviors through suppressing NF-κB and NLRP3 signaling pathway. Brain Res Bull 142:352-359.

Zhao R, Ying M, Gu S, Yin W, Li Y, Yuan H, Fang S, Li M (2019) Cysteinyl leukotriene receptor 2 is involved in inflammation and neuronal damage by mediating microglia M1/M2 polarization through NF-κB pathway. Neuroscience 422:99-118.

Zhou K, Zhong Q, Wang YC, Xiong XY, Meng ZY, Zhao T, Zhu WY, Liao MF, Wu LR, Yang YR, Liu J, Duan CM, Li J, Gong QW, Liu L, Yang MH, Xiong A, Wang J, Yang QW (2017) Regulatory T cells ameliorate intracerebral hemorrhage-induced inflammatory injury by modulating microglia/macrophage polarization through the IL-10/GSK3β/PTEN axis. J Cereb Blood Flow Metab 37:967-979.

C-Editor: Zhao M; S-Editors: Yu J, Li CH; L-Editors: Giles L, Yu J, Song LP; T-Editor: Jia Y